JOURNAL OF MATERIALS SCIENCE 10 (1975) 1608–1615

Thermal fracture studies in ceramic systems using an acoustic emission technique

A. G. EVANS
Science Center, Rockwell International, Thousand Oaks, California, USA

M. LINZER, H. JOHNSON
Inorganic Materials Division, National Bureau of Standards, Washington, D.C., USA

D. P. H. HASSELMAN, M. E. KIPP
Materials Research Center, Lehigh University, Bethlehem, Pennsylvania, USA

An acoustic emission technique for measuring the failure time in thermal shock experiments is described. The technique offers a unique opportunity to measure the heat-transfer coefficient of the test system and hence, to obtain a fully quantitative measure of the peak surface stress generated during the test. Measurements on soda-lime glass have demonstrated that rapid thermal fracture in the material occurs when the surface stress attains a critical value equal to the propagation stress for the most deleterious surface flaw. The effects of slow crack growth on the failure time are also investigated and correlated with recently developed theory.

1. Introduction

Thermal fracture, especially under transient cooling conditions (thermal shock), is one of the primary failure modes in ceramic systems. However, because it is such a complex phenomenon, our current understanding of this fracture process is still rather rudimentary. A complete evaluation of the problem requires a specific understanding of the two primary stages in the fracture process; (a) the critical condition for the onset of rapid fracture, which determines the onset of strength degradation, (b) the condition for crack arrest, which determines the magnitude of the strength degradation. The former problem is addressed in this paper; the latter has been examined in a separate study [1].

The most comprehensive treatment of the onset of rapid fracture has been conducted by Hasselman [2]. He has essentially utilized fracture mechanics concepts by considering that rapid fracture will commence when the critical stress intensity factor, K_{IC}, at the most deleterious flaw (corresponding to the critical flaw propagation stress, σ_c) has been exceeded. More recently, the treatment has been extended to incorporate the effects of slow crack growth at $K_I < K_{IC}$ [3]. The existing theory contains, however, certain assumptions which have not been directly verified. Specifically, it is assumed that [2, 3] (a) the stress along the initial crack trajectory (prior to rapid propagation) is uniform and equal to the maximum tensile stress at the component surface, and (b) the isothermal slow crack growth data accurately characterizes the slow crack growth under variable temperature conditions. The primary purpose of this paper is to describe an acoustic emission technique which can be used to quantitatively determine the condition for the onset of rapid fracture and hence, to assess both the general validity ofthe critical stress intensity factor approach and the aptness of the assumptions used in the existing theory.

2. The onset of rapid crack propagation

Existing theory [2, 3] for the onset of rapid fracture simply considers that the stress* acting over the length of the pre-existing crack is

*This stress is the normal stress that would exist at the crack plane in the absence of the crack; this is the stress that is used to calculate K_I – using a Green's function in conjunction with the principle of superposition [4].

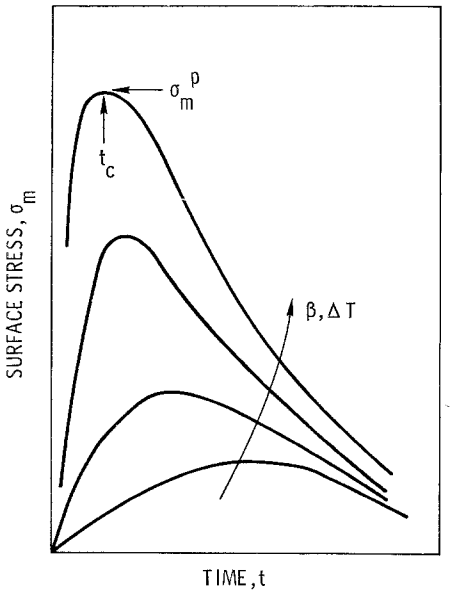

Figure 1 A schematic drawing showing the variation of the surface stress with time in a quench test.

uniform and equal to the maximum stress at the component surface, σ_m. Hence, for a critical stress intensity factor (or a critical flaw propagation stress) criterion, rapid fracture occurs when

$$\sigma_m = \frac{K_{IC}}{Y\sqrt{a_0}}$$

or

$$\sigma_m = \sigma_c \qquad (1)$$

where a_0 is the initial flaw size and Y is a geometric factor. The stress varies with time [5], as shown schematically in Fig. 1, and exhibits a peak, σ_m^P, at some time t_c after the imposition of the temperature differential, ΔT. The magnitude of the peak stress is given in general by [5, 6];

$$\sigma_m^P = \frac{E\alpha\Delta T}{(1-\nu)} B(\beta) \qquad (2)$$

where E is Young's modulus, α is the linear thermal expansion coefficient, ν is Poisson's ratio and β is the Biot modulus, defined as

$$\beta = \frac{Rh}{k} \qquad (3)$$

where R is a specimen dimension, h is the heat-transfer coefficient and k is the thermal conductivity of the specimen. The function $B(\beta)$ depends on the specimen configuration, and usually increases as β increases. For a sphere [6]

$$B(\beta) \approx \frac{2\beta}{5(\beta+2)} \qquad 0.1 < \beta < 10$$

$$B(\beta) \approx 1 - (6/\pi\beta)^{1/2} \qquad \beta \gg 10\,. \qquad (4)$$

Equating σ_m^P to σ_c (Equation 1) gives the critical temperature differential ΔT_c, for the onset of rapid fracture:

$$\Delta T_c = \frac{\sigma_c(1-\nu)}{E\alpha B(\beta)} \equiv \frac{\sigma_m^P(1-\nu)}{E\alpha B(\beta)}\,. \qquad (5)$$

In principle, therefore, it is possible to predict ΔT_c for a body with a known σ_c. In practice, however, gross uncertainties are usually involved because the heat-transfer coefficient, h, which determines β, is not known with any significant precision. The difficulties in assigning a value for h are due to the strong dependencies of h on ΔT, the turbulence of the medium, the incidence of boiling, the shape of the body, etc. For example, for a hot metal wire in water [7], h varies by four orders of magnitude, from 0.013 to 13 cal g^{-1} cm^{-2} $°C^{-1}$, sec^{-1} as ΔT varies from 20 to 400° C.

A detailed comparison of the predictions of the thermal fracture theory with experimental observations demands, therefore, that the measured quantity does not depend on a determination of h. An approach which has this desirable feature measures the time taken for the onset of rapid fracture, after the initial exposure to the cooler ambient. Consider a series of experiments in which the temperature differential imposed on a body is incrementally increased until rapid crack propagation commences. At this critical condition, the time taken for rapid fracture to occur must coincide with the time, t_c, taken for the stress to attain the peak value, provided that slow crack growth effects are eliminated. The time at the peak stress is given in general by [5, 6];

$$t_c = \frac{R^2}{k} \rho C B'(\beta) \qquad (6)$$

where ρ is the density and C the specific heat of the body and $B'(\beta)$ is a function of β that initially increases very rapidly with β and then decays, as shown in Fig. 2 for a spherical configuration [6]. By treating Equations 6 and 2 as a pair of simultaneous equations, β can be eliminated and an expression relating t_c and $\sigma_m^P/\Delta T$ can be obtained. A typical curve relating these two

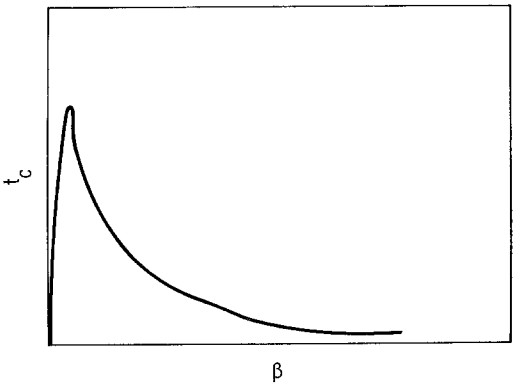

Figure 2 A schematic showing the effect of the Biot modulus, β, on the time when the surface stress reaches its peak value, t_c.

variables, calculated for soda-lime-silicate glass spheres, using the exact solutions of Carslaw and Jaeger [8] and Boley and Weiner [9], is shown in Fig. 3 (the physical property data and the equations used to evaluate this curve are listed in Table I). The curve has two branches: for large $\sigma_m{}^P/\Delta T$ (corresponding to large β), the critical time increases as the peak stress decreases; for very small $\sigma_m{}^P/\Delta T$ (very small β), t_c decreases as $\sigma_m{}^P$ decreases. However, only the upper branch shown in Fig. 3 need be considered for β values of practical importance.

TABLE I Physical property data for soda-lime glass used in calculating thermal fracture effects

Coefficient of thermal expansion (α)	9.3×10^{-6} °C^{-1}
Young's modulus (E)	6.9×10^{1} MN m^{-2}
Poisson's ratio (ν)	0.25
Thermal conductivity (k)	2.5×10^{-1} cal °C^{-1} sec^{-1} m^{-1}
Specific heat (C)	0.22 cal g^{-1} °C^{-1}
Density (ρ)	2.53×10^{6} g m^{-3}
Sphere radius (R)	3.2×10^{-3} m
Critical stress intensity factor, K_{IC}	0.75 MN m$^{-3/2}$

It is apparent from Fig. 3 that an experimental determination of the time taken for the onset of rapid fracture at the critical condition – which is then coincident with t_c – gives directly a value for the ratio of the peak surface stress to the critical temperature differential $\sigma_m{}^P/\Delta T_c$. No assumptions regarding the appropriate value for β are needed; in fact, the measurement of t_c can give a direct measure of β for the actual test conditions. By also measuring the temperature differential for the test, ΔT_c, the ratio $\sigma_m{}^P/\Delta T_c$ can be converted into an absolute measure of the peak stress $\sigma_m{}^P$. This value of the peak stress can then be compared with an independently

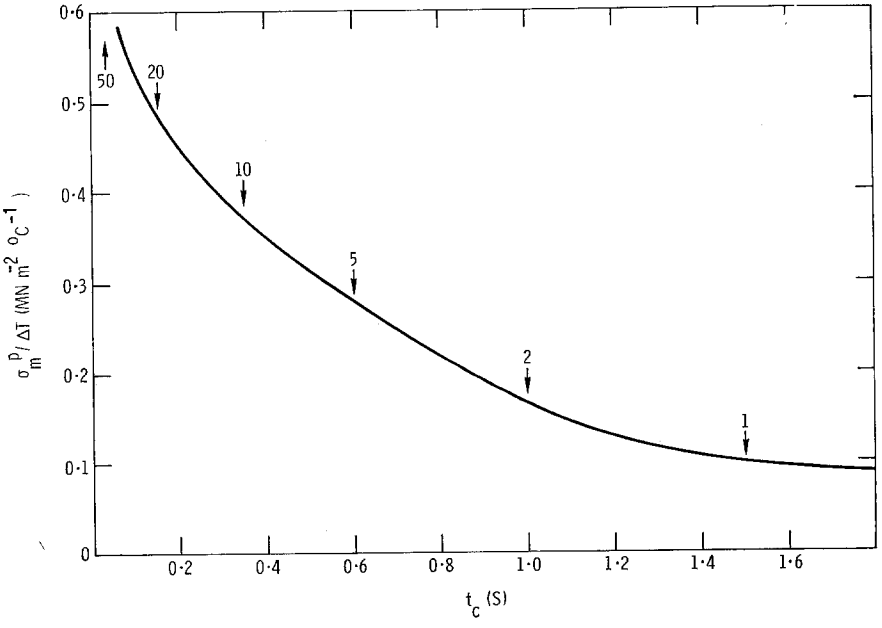

Figure 3 The relationship between the time of the peak stress and the peak surface stress for soda-lime glass sphere, 3.2×10^{-3} m diameter.

determined value for the crack propagation stress, σ_c.

3. The acoustic emission technique

3.1. The concept

Several prior studies in ceramic systems [10, 11] have indicated that acoustic emission is a very sensitive measure of crack propagation events, both microcracking and macrocrack growth. Each cracking event emits stress waves which are transmitted to a transducer and transformed into a voltage which, for a high-Q transducer, usually exhibits the characteristic form of a damped sinusoid. The magnitude of the voltage output (either the peak voltage or the number of times that the voltage crosses a preset threshold) gives a direct measure of the crack-length increment that constituted the event [10, 12]. Independent studies by the authors have also indicated that the impact of a falling sphere as it progresses through the surface of a liquid is accompanied by stress waves, which can be detected by a transducer attached to the outside of the container. Hence, a system with good time resolution and the ability to distinguish the separate emissions from the surface impact and the crack propagation events, would permit the time taken for the onset of crack growth to be measured.

3.2. Instrumentation

The acoustic emission system previously reported [10] was upgraded by the addition of a videotape recorder. This allowed us to record the acoustic emission signals for subsequent processing and analysis. The recorder had stop-action playback, > 40 dB dynamic range and an upper frequency limit of about 3 MHz. It was modified for analog signal recording as described by Reis [13]. In addition, a gating circuit with variable width and delay was constructed which enabled us to focus on individual bursts for frequency and amplitude analysis. The frame duration was 17 msec and, by displaying the gated frame signal on a standard oscilloscope, resolutions of < 10 μsec on burst separation could easily be achieved when no signal overlap occurred.

3.3. Analysis

Our first objective was to determine whether the transducer response to the impact event and the crack growth event can be readily discerned and distinguished. This was assessed by initially dropping small spheres at ambient temperature into a liquid within a container and noting the response of a broad band transducer (Dunegan/Endevco Model S9201) located on the outside of the container, adjacent to the surface of the liquid. By interposing a layer of foam rubber between the liquid and the container, we found that the impact could be characterized by a single signal, with a dominant frequency of ~ 50 kHz (Fig. 4a). Another single signal was obtained when the sphere contacted the bottom of the container. Hence, the total time of descent through the liquid could be determined, and compared with independent (direct) measurements to confirm that the signals were coincident with the impact events.

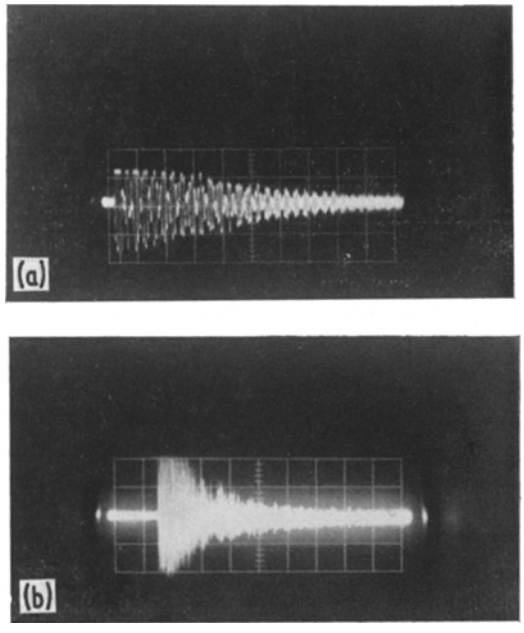

Figure 4 (a) A typical acoustic emission signal for a sphere impacting the surface of a liquid. (b) A typical acoustic emission signal corresponding to a rapid crack propagation event.

In a subsequent series of experiments, pre-heated spheres were dropped into the same liquid/container system. After each test, the acoustic emission signals were examined, and the spheres were inspected for cracks using transmission optical microscopy. For glass spheres, large amplitude signals (Fig. 4b) with a dominant frequency of 1 MHz were obtained whenever macrocracks were detected. Close inspection revealed a direct correlation between the number of signals (excluding the two impact signals) and the number of macrocracks. For several other

materials, notably porcelain and lucalox (sintered alumina), many more acoustic emission signals were apparent and there was no correlation between the number of signals and the number of macrocracks. These observations are consistent with other studies [10, 11] which have indicated that extensive acoustic emission occurs in porcelain and lucalox prior to rapid macrocrack propagation, due to the formation of non-propagating microcracks and the slow propagation of macrocracks; whereas for glass, acoustic emission is only obtained from the rapid propagation of macrocracks. Hence, glass is the ideal material for the proposed study of the critical time for the onset of rapid macrocrack propagation. Additional simplicity is afforded by the marked difference in the dominant frequency characteristics of the impact and crack growth events.

3.4. Test procedure

Two quench media were selected for this study, degassed silicone oil and water. The oil was selected primarily to avert the complexities that might result from slow crack growth. The results from these tests will be used directly to assess the validity of the critical stress criterion for rapid crack propagation. The tests in water were conducted to afford a measure of the importance of slow crack growth.

Initially, an approximate critical temperature for rapid crack propagation was experimentally determined for each test medium using pre-cracked spheres (see below). Then, for the tests in silicone oil, each sphere was initially quenched from a temperature just below this approximate value. If macrocrack propagation did not occur, quenching was continued, by incrementally increasing the pre-heat temperature, until macrocrack propagation was detected. This procedure gave very precise values for ΔT_c and t_c. For the tests in water, this procedure was modified because each subcritical quench might have produced some crack extension by slow crack growth. Instead, each sphere was quenched only once, from a temperature just below the approximate value determined previously using another set of pre-cracked spheres. Under these conditions only a small proportion of the spheres were expected to develop macrocracks, and it was recognized that for those spheres that did

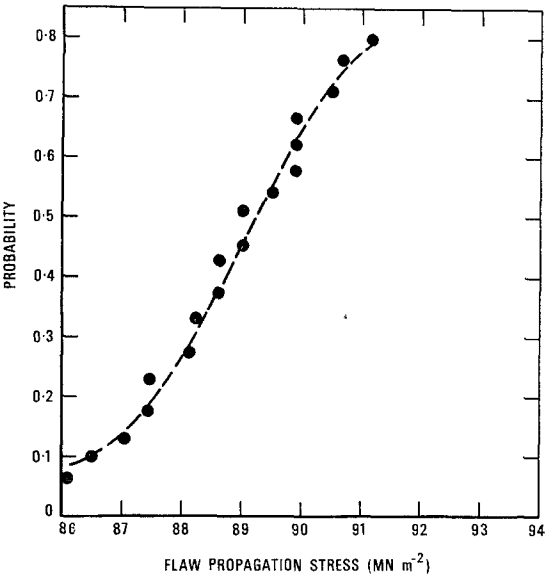

Figure 5 The biaxial flaw propagation stress for soda-lime glass discs, indented with 200 g Knoop indentation, tested in dry nitrogen gas.

crack, the imposed temperature must, to some small extent, be supercritical.

4. The flaw propagation stress

The pre-existing flaws in ceramic materials generally exhibit a wide statistical size distribution, which leads to a corresponding distribution in σ_c. The characterization of the σ_c distribution – which is required for the proposed comparison with the peak surface stress – is an exacting task (especially in a spherical configuration) which is not merited for the present study. It is more satisfying to introduce artificial flaws larger than the pre-existing flaws, which are readily amenable to characterization. The Knoop microhardness indentation technique [16] which generates controlled semi-elliptical surface flaws in ceramic materials, is ideal for this purpose, and was used in these studies.

The flaws introduced by the indentation can be characterized in terms of their extension stress by alternately indenting a series of biaxial flexure discs* and spheres (of the same composition) and measuring the flaw propagation stress, i.e. the fracture stress, on the discs in a dry nitrogen gas environment (which eliminates slow

*Biaxial tension (1:1) is used because the stress state in the thermal shock tests is also a 1:1 biaxial tension.

TABLE II Times taken for rapid crack propagation

1. Oil quench

(a) Pre-cracked – critical

	Temperature differential (°C)					
	246	248	250	245	245	254
Time for rapid crack propagation (sec)	0.31	0.22	0.35	0.28	0.38	0.32

(b) No pre-cracks

	Temperature differential (°C)		
	450	480	500
Time for rapid crack propagation (sec)	0.1, 0.25	0.02, 0.1, 0.4	0.002, 0.03, 0.1, 0.11, 0.8

2. Water quench

(a) Pre-cracked – supercritical

	Temperature differential (°C)		
	120	120	120
Time for rapid crack propagation (sec)	0.10, 0.16	0.18, 0.25	0.06, 0.15, 0.16 0.20

crack growth), using an apparatus described by Wachtman *et al.* [15].

5. Results

A Knoop indentation using a 200 g load generated consistent surface cracks ($\sim$ 20 μm in diameter) emanating from the corners of the indentation. The biaxial flexture strength results for twenty indented specimens, plotted in Fig. 5, give a median flaw extension stress of 90 MN m^{-2}.

The results of the critical time measurements are summarized in Table II. Good consistency was obtained for the tests in oil. Only one cracking event was detected, the critical temperature varied from 244 to 254°C (average 248°C) and the critical time varied from 0.22 to 0.38 sec (average 0.3 sec). The tests in water were less satisfying. For a quench temperature of 120°C, about 10% of the spheres developed cracks, but crack propagation occurred in several steps ranging from 0.06 to 0.25 sec (average 0.15 sec) with a substantial variation in the time separation within the propagation sequence.

A few tests in silicon oil for spheres without pre-cracks are also presented in Table II. These illustrate the marked effect of the initial flaw size on the critical temperature and the sequential nature of crack propagation when several cracks have been activated.

6. Discussion

The median value for the crack propagation time measured using the silicone oil quench medium (0.31 sec), gives a value for $\sigma_m{}^P/\Delta T$ (from Fig. 3) of 0.38 MN m^{-2} °C^{-1} (corresponding to a Biot's modulus of $\sim$ 12, or a heat-transfer coefficient of 0.095 cal cm^{-2} sec^{-1} °C^{-1}). Combining this with the measured critical temperature of 248°C gives a maximum surface stress during the quench of 94 MN m^{-2}. This compares rather favourably with the median critical flaw propagation stress of 90 MN m^{-2}, measured in the biaxial flexure tests. We conclude, therefore, that the onset of rapid crack propagation under a thermal shock condition is well described by a critical flaw propagation criterion, based on the maximum stress developed at the component surface – at least for surface flaws within the size range used in this study (up to $\sim$20 μm).

For the analysis of the water quench tests we shall just consider the first rapid macrocrack growth event.* The critical time for the first

*The subsequent events are almost certainly related to the supercritical nature of the temperature of the quenches, which causes the first crack to propagate before the peak stress is reached. Crack propagation events can then continue, until the peak stress is reached.

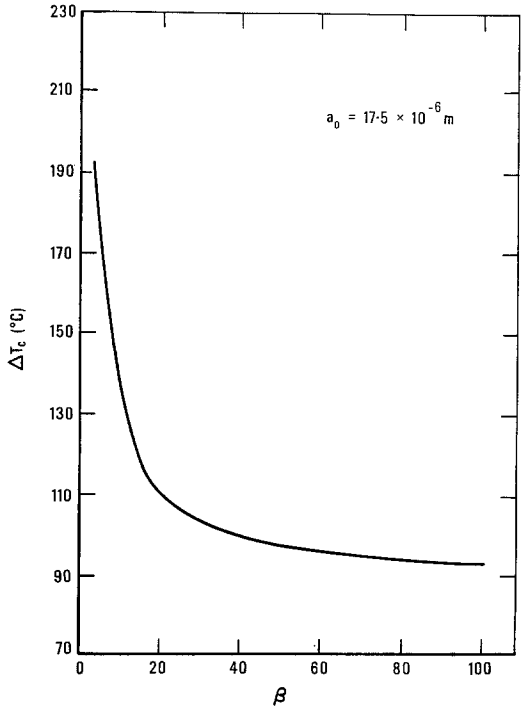

Figure 6 The relation between the critical temperature differential, ΔT_c, and Biot's modulus, β, for soda-lime glass sphere containing a surface pre-crack 17.5 μm in depth, quenched into water.

propagation event and the critical temperature can again be used to determine a value for the maximum surface stress from Fig. 4. This procedure yields a stress, 66 MN m^{-2}, which is substantially below the critical flaw propagation stress of 87 MN m^{-2}, at the equivalent failure probability*. A consistent description of the onset of rapid crack propagation in a water quench is not, therefore, provided by equating the peak value of the surface stress to the critical flaw propagation stress. Since the apparent peak stress is lower than the critical flaw propagation stress, the disparity is almost certainly attributable to slow crack growth. Hence, we propose to analyse the onset of rapid propagation by incorporating the slow crack growth effect – using the computer code developed by Badaliance *et al.* [3] – to determine whether a consistent description then emerges. The calculation commences with a value for the initial flaw size, a_0. For a surface crack, an apparent a_0 can be inferred from the flexural crack propagation stress, using the relation [3];

$$a_0 = \frac{K_{IC}^2}{1.28\pi\sigma^2} \equiv \frac{K_{IC}^2}{Y^2\sigma^2}. \quad (7)$$

At the 10% probability level, the apparent a_0 is 17.5×10^{-6} m. This value for a_0, in conjunction with slow crack growth data for soda-lime glass in water [14], may first be used to calculate a relation between the critical temperature differential, ΔT_c, and Biot's modulus, β. The $\Delta T_c/\beta$ curve is shown in Fig. 6. Noting that the critical temperature for the water quench must be approximately 120° C, we obtain from Fig. 6 an approximate value for β of 13, i.e. a heat-transfer coefficient, $h \approx 0.1$ cal sec^{-1} m^{-1} °C^{-2}. This value for h falls nicely within the range, 0.015 to 0.15 cal sec^{-1} m^{-2} °C^{-1}, obtained at this temperature differential by Farber and Scorah [7]. Next, we calculate the relation between the failure time, t_f, and the temperature excess, ΔT-ΔT_c, for this value of β, as shown in Fig. 7.

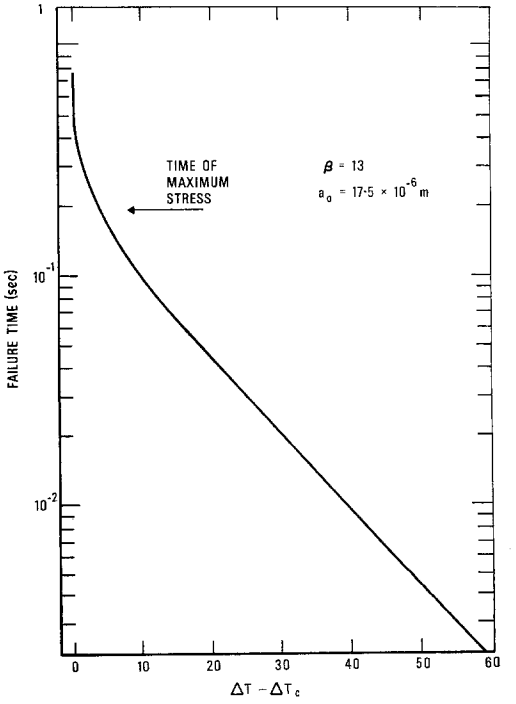

Figure 7 The relation between the failure time, t_f, and the temperature excess, ΔT-ΔT_c, for soda-lime glass spheres with a 17.5 μm surface pre-crack, quenched into water, and assuming a value for β of 13.

*Only 10% of the spheres developed macrocracks in the thermal shock experiments and hence, the appropriate crack propagation stress to use for comparison is the stress at the 10% failure probability level (see Fig. 6).

The magnitude of the temperature excess in the water quench tests is not accurately known, but due to the relatively narrow distribution in the flaw propagation stress (Fig. 5), we estimate that it is unlikely to exceed 5° C. The times for the onset of rapid crack propagation (Fig. 7) should thus be in excess of 0.15 sec. The measured times, for the first event (Table II), are mostly somewhat shorter than the predicted times and hence, the observed behaviour is not entirely consistent with the existing crack propagation model.

The disparity is not large, however, and it may simply be related to an incorrect assignment of the numerical values for the important fracture mechanics and thermal parameters. For example, by simply changing the flaw geometry parameter, Y, from the value used here – for a long surface crack – to a larger value more typical of a semi-elliptical surface crack, the failure time for a 5° C temperature excess decreases to 0.12 sec, which is significantly closer to the measured failure times.

Thus, we conclude that the existing crack propagation model for thermal fracture [3] is reasonably consistent with failure times observations for soda-lime glass in water quench tests.

7. Summary and conclusions

We have described an acoustic emission technique which can be used to give a quantitative measure of both the heat-transfer coefficient and the time for rapid crack propagation in quench tests. Measurements of the failure time for pre-cracked soda-lime glass spheres in oil quench tests have shown that the critical crack propagation stress criterion for the onset of rapid fracture in thermal shock tests is entirely valid in the absence of significant slow crack growth, at least for flaws < 20 μm in depth. Failure time measurements in water quench tests have indicated that slow crack growth can exert a major influence on the conditions for the onset of rapid crack growth. Additionally, reasonable consistency with a model by Badaliance *et al.*, for rapid crack propagation preceded by slow crack growth, has been demonstrated for the soda-lime glass/water system.

Acknowledgements

A.G.E. wishes to acknowledge the Aeronautics Research Laboratory for their support. D.P.H.H. wishes to thank the Army Research Office for support under contract DA-ARO-D-31-124-73-G45.

References

1. E. R. FULLER and A. G. EVANS, *Met. Trans.*, to be published.
2. D. P. H. HASSELMAN, *J. Amer. Ceram. Soc.* **52** (1969) 600.
3. R. BADALIANCE, D. A. KROHN and D. P. H. HASSELMAN, *ibid*, **57** (1974) 432.
4. G. C. SIH, "Handbook of Stress Intensity Factors" (Lehigh University, Bethlehem, Pa., 1973).
5. W. D. KINGERY, *J. Amer. Ceram. Soc.* **38** (1955) 3.
6. W. B. CRANDALL and J. GING, *ibid* **38** (1955) 44.
7. E. A. FARBER and R. L. SCORAH, *Trans. ASME* **70** (1948) 369.
8. H. S. CARSLAW and J. C. JAEGER, "Conduction of Heat in Solids" (Oxford University Press, Oxford, 1959).
9. B. A. BOLEY and G. H. WEINER, "Theory of Thermal Stress" (Wiley, New York, 1960).
10. A. G. EVANS and M. LINZER, *J. Amer. Ceram. Soc.* **56** (1973) 575.
11. A. G. EVANS, M. LINZER and L. R. RUSSELL, *Mater. Sci. Eng.* **15** (1974) 253.
12. A. J. POLLOCK, *Non-Destructive Testing*, October (1973) p. 266.
13. J. J. REIS, *Research/Development*, February (1972) p. 24.
14. J. J. PETROVIC, L. A. JACOBSON and P. J. TALTY, *J. Amer. Ceram. Soc.*, **58** (1975) 113.
15. J. B. WACHTMAN, JUN, W. CAPPS and J. MANDEL, *J. Mats.* **7** (1972) 188.
16. S. M. WIEDERHORN and L. H. BOLTZ, *J. Amer. Ceram. Soc.* **53** (1970) 543.

Received 4 December 1974 and accepted 23 January 1975.